Acta Crystallographica Section A
Foundations and Advances
ISSN 2053-2733

Received 11 July 2014
Accepted 3 September 2014

High-symmetry embeddings of interpenetrating periodic nets. Essential rings and patterns of catenation

Charlotte Bonneau[a] and Michael O'Keeffe[b]*

[a]Glencroft, Guildford, Surrey, England, and [b]Department of Chemistry and Biochemistry, Arizona State University, 1604, Tempe, AZ 86287, USA. Correspondence e-mail: mokeeffe@asu.edu

Symmetrical embeddings are given for multiply intergrown sets of some commonly occurring nets such as **dia** (diamond), **qtz** (quartz), **pcu** (net of primitive cubic lattice) and **srs** (labyrinth net of the *G* minimal surface). Data are also given for all known pairs of nets which have edge-transitive self-dual tilings. Examples are given for symmetrical polycatenation of the 2-periodic nets **sql** (square lattice) and **hcb** (honeycomb). The idea that the rings that are the faces of natural tilings form a complete basis set (essential rings) is explored and patterns of catenation of such rings described.

1. Introduction

An important and fascinating aspect of crystal chemistry is the fact that in many instances the underlying nets of crystal structures are entangled in some way. In what is perhaps the simplest kind, two or more identical copies of a net are intergrown so that rings of one net are catenated with those of other copies (*e.g.* Batten & Robson, 1998; Carlucci *et al.*, 2003, 2014; Blatov *et al.*, 2004). Such structures are the topic of this paper. From the mathematical point of view, the subject is challenging. Conventional graph theory knows nothing of knots and entanglements although *spatial* graph theory [which deals with embedded graphs and such properties as knottedness (Hyde & Delgado-Friedrichs (2011)] is a subject of active research with applications to biological structures (*e.g.* Forgan *et al.*, 2011). The simplest kind of entanglement occurs in catenanes in which molecules, otherwise unconnected, are joined as links in a chain (*catenated*). The study of such structures remains a topic of considerable chemical interest (*e.g.* Niu & Gibson, 2009; Evans & Beer, 2014). The first molecular catenanes were produced in small yield over 50 years ago (Wasserman, 1960). It was not generally realized by chemists that in fact one of the first crystal structures ever determined, that of cuprite (Cu_2O; Bragg & Bragg, 1915), consists of two interpenetrating networks in which O atoms joined by –Cu– links form two diamond nets in which each ring is catenated to six others (Fig. 1). The structure of cuprite was clearly described and illustrated as interpenetrating nets in the first *Strukturbericht* (Ewald & Hermann, 1931).[1] In the same volume one can find a description of the $MgCu_2$ structure as interpenetrating nets of two different kinds.

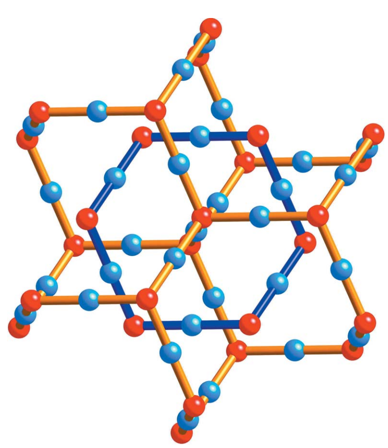

Figure 1
Part of the Cu_2O structure (O red, Cu blue) showing a Cu_6O_6 ring catenated with six others.

The aim of this paper is to provide coordinates for high-symmetry embeddings of non-intersecting intergrown nets and to examine the patterns of catenation of rings. It is not a review of crystal structures, which are only incidentally cited. The subject is of practical importance for porous materials and conscious efforts may be made either to encourage or to deter such intergrowth in practical materials (Reineke *et al.*, 2000). Knowledge of possible symmetries can also be of assistance in structure elucidation (Uribe-Romo *et al.*, 2009). Nets based on interpenetrating nets joined by extra links have some interesting embeddings in which those links have zero length (Delgado-Friedrichs *et al.*, 2013).

[1] 'Der C3-Typ hat die interessante Eigenschaft, dass allein kürzeren Verbindungen *d* schon eine dreidimensional unendliche Atommenge zusammenfassen, die aber trotzdem noch nicht alle Atome des Kristalls enthält. Die Atommengen, die allein durch die Verbindungen *d* zusammengefasst werden, bilden zwei Gitter des C9-Typs, die einander durchdringen, ohne ein Atom miteinander gemeinsam zu haben.' (The C3-type [cuprite] has the interesting property that the shortest connections *d* alone span a three-dimensional infinite set of atoms, which nonetheless does not contain all atoms in the crystal. Those atom sets which are spanned by the connections *d* alone constitute two lattices of type C9 which interpenetrate each other without having any atom in common.)

A pair of interpenetrating nets are separated by a periodic surface and some of these, notably the gyroid (or G) surface, are of considerable interest in materials science (Hyde *et al.*, 2008). Recently, attention has also been directed at the multi-continuous surfaces separating sets of three or more interpenetrating nets (Schröder-Turk *et al.*, 2013), so knowledge of possibilities for such structures is also relevant in this context.

The nets we are concerned with are *stable*, *i.e.* do not have collisions (overlap) between vertices in barycentric coordinates. For such nets the graph automorphism group is isomorphic to a crystallographic space group (Delgado-Friedrichs, 2005; Moreira de Oliveira & Eon, 2014), so we seek embeddings in that symmetry. For high-symmetry nets like that of diamond only two copies of full symmetry can be obtained. For multiple copies the most symmetrical embedding is chosen. In an embedding the *vertices* and *edges* of the abstract net are referred to as *nodes* and *links*, respectively. A requirement is that nodes do not overlap and that straight links do not overlap or intersect. Nets are identified by a three-letter RCSR (Reticular Chemistry Structure Resource) symbol such as **xyz** (O'Keeffe *et al.*, 2008). For a catenated pair of nets an extension is added such as **xyz-c**. **xyz-c***n* indicates there are n identical copies of the net intergrown. For space groups with two origin choices in *International Tables for Crystallography*, the second choice (origin at an inversion center) is always used. Data for structures are given in *Systre*-readable files in the supporting information.[2] *Systre* (Delgado-Friedrichs & O'Keeffe, 2005) determines the degree of interpenetration.[3]

Mention should be made of complementary work by Koch *et al.* (2006), in which interpenetrating sphere packings were enumerated and described. In sphere-packing nets the shortest distance between nodes corresponds to links – a situation that occurs for only one of the structures (**srs-c**) considered here.

A classification of embeddings following Blatov *et al.* (2004) is: class I, components related by translation; class II, components related by other symmetry operations; class III, components related by a combination of translations and other symmetry operations. This classification is usually applied to embeddings actually found in crystal structures, which may be different from the maximum-symmetry embeddings reported herein. Embeddings of interpenetrating nets may be further characterized according to whether they preserve the full symmetry of the net. Thus in embeddings of the diamond net discussed below, there is an embedding of two interpenetrating diamond nets that preserves the full cubic symmetry, but embeddings of intergrowths of three or more have at most tetragonal symmetry for the individual net.

The ultimate goal of the net taxonomist is to classify interpenetrations so that any two can be said to be the same or different. In this regard one might consider two interpenetrations the same if they are *ambient isotopic*. Two embeddings are ambient isotopic if one can be deformed into the other without links passing through each other. Structures with the same topology but not ambient isotopic have been called *isotopes* (Castle *et al.*, 2011).

Distinct isotopic interpenetrations can be distinguished by finding a *Hopf ring net* (HRN) (Alexandrov *et al.*, 2012); we give an example below. Unfortunately, as the authors note, structures with the same HRN are not necessarily ambient isotopic.

2. Rings, tilings and essential rings

The nets most prone to interpenetration are those with self-dual natural tilings.[4] In this case the nodes of a second net fit in the interstices (tiles) of the first and *vice versa*. It is not surprising that the three regular nets with this property (**srs**, **dia** and **pcu**) are those most commonly occurring in crystal structures with disjoint components (Blatov *et al.*, 2004; Alexandrov *et al.*, 2011) and our attention is particularly focused on those nets. For such structures, each n-ring of one net will be catenated with n-rings of the second net. n = 10, 6 and 4 for **srs**, **dia** and **pcu**, respectively.

A net contains an infinite number of cycles (a closed path along edges); only a small set of those, a finite number per vertex, are of relevance to describing catenation – but just what are they? First, we note that there is only a finite number of *rings* and *strong rings* per vertex. A ring is defined as a cycle that is not the sum of two smaller cycles and a strong ring is defined as a cycle that is not the sum of any number of smaller cycles (Goetzke & Klein, 1991; Delgado-Friedrichs & O'Keeffe, 2005).[5] The faces of convex polyhedra are rings, but not necessarily strong rings; the 4-ring base of a square pyramid is a ring but not a strong ring (it is the sum of the four 3-rings of the other faces). A ring that is not strong is called *weak* (Blatov *et al.*, 2007) and we use that term here.

If a net admits a natural tiling (Blatov *et al.*, 2007), the faces are strong rings in at least the local sense that, by definition, there is not one tile face that is larger than the rest. But not all strong rings are faces of tiles in a given tiling – only a subset, which we have called the *essential rings* of the structure (Delgado-Friedrichs *et al.*, 2003). We conjecture that the rings so selected form a complete basis set in the sense that all other cycles can be expressed as a sum of these. We note, however, that not all nets admit a tiling; for these, a basis set of essential rings can still be identified. On the other hand, if a net does admit a tiling the essential rings are not catenated ('self-entangled'), so that many nets such as **coe** (net of coesite) which have been described as self-catenated (O'Keeffe, 1991) but which admit a natural tiling should perhaps not be so

[2] Supporting information for this paper is available from the IUCr electronic archives (Reference: EO5041).

[3] *Systre* is freely available at http://www.gavrog.org.

[4] A *natural* tiling has the same symmetry as the intrinsic symmetry of the net (Delgado-Friedrichs *et al.*, 2003). Except as noted, this is a unique tiling for the nets considered in this paper.

[5] The sum of two rings consists of those edges that occur once; the sum of a set of rings consists of those edges that occur an odd number of times. A face of a polyhedron (or generalized polyhedron such as a three-dimensional tile) is the sum of all the other faces.

Table 1
Parameters for maximum-symmetry embeddings of **dia** (diamond) nets.

The edges are of unit length, and for the tetragonal structures the coordination figure is a regular tetrahedron. In the first column, N is the number of component nets and n is any integer.

N	Space group	a	c	a/c	Node	Link
1	$Fd\bar{3}m$	$4/3^{1/2}$	a	1	1/8, 1/8, 1/8	to −1/8, −1/8, −1/8
2	$Pn\bar{3}m$	$2/3^{1/2}$	a	1	1/4, 1/4, 1/4	to −1/4, −1/4, −1/4
$2n$+1	$I4_1/amd$	$(8/3)^{1/2}$	$4/3^{1/2}N$	$N/2^{1/2}$	0, 3/4, 1/8	to 0, 5/4, $1/8 + (-1)^{(N+1)/2}N/4$
$4n$	$P4/nbm$	$2/3^{1/2}$	$4/3^{1/2}N$	$N/2$	3/4, 1/4, 0	to 1/4, 3/4, $-(-1)^{N/4}N/4$
$4n$+2	$P4_2/nnm$	$2/3^{1/2}$	$4/3^{1/2}N$	$N/2$	3/4, 1/4, 1/4	to 1/4, 3/4, $1/4 + (-1)^{(N+2)/4}N/4$

described. For the **qtz** (quartz) net, discussed below, the set of essential rings is smaller than the set of strong rings.

The essential rings are similar in some ways to the smallest set of smallest rings (SSSR) used by molecular chemists or, more generally, the minimum cycle basis (MCB) used in other areas of applied graph theory (*e.g.* Lee *et al.*, 2009, and references therein), but there are differences. A molecule has a finite number of cycles and the SSSR is a minimal basis set such that all other cycles are a sum of some, or all, of the basis cycles. Thus the molecule cubane whose graph (omitting H atoms) is that of a cube is considered to have just five rings (the sixth face of the cube is the sum of the other five) and the (partial) IUPAC name is pentacyclooctane. On the other hand, in the net of the primitive cubic lattice which is carried by a tiling of cubes, there are three 4-rings per vertex and we do not take into account the fact that each ring is the sum of five others.

The set of essential rings, as defined by a natural tiling, is not always minimal. Thus consider the natural tile of the net **lcy** (discussed further below) shown in Fig. 2. If the skeleton of the tile were the graph of a molecule, the molecule would be considered tricyclic (one 3-ring and two 5-rings). However, we prefer to consider two families of rings – one 3-ring and three 5-rings per vertex. If we wanted a truly minimal basis we could exclude the 3-rings as sums of 5-rings.

3. Families of intergrown 3-periodic nets

3.1. The dia (diamond) and ths nets

The diamond net is cubic, with symmetry $Fd\bar{3}m$. Two interpenetrating diamond nets displaced by **a**/2 (original cell) have symmetry $Pn\bar{3}m$ with each net having the full symmetry. For more interpenetrating nets, the maximum symmetry is tetragonal with individual nets of symmetry $I4_1/amd$ (site symmetry at a node $\bar{4}m2$). The symmetry of the most symmetrical embedding, with nets related by translation **c**, depends on the number of components, N (Uribe-Romo *et al.*, 2009). For N odd, the symmetry is $I4_1/amd$. For N twice an even number, the symmetry is $P4/nbm$, and for N twice an odd number, it is $P4_2/nnm$. Explicit coordinates for the most symmetrical configuration and regular tetrahedral coordination are given in Table 1. All the links are related by symmetry, so it is enough to specify one. Each ring is catenated with $6(N-1)$ others. Blatov *et al.* (2004) give examples of crystal structures with these class-I interpenetrations for N = 2–10.

It is worth noting that one can have a cubic structure of threefold interpenetrating diamond nets of class II, if the coordination figure at the vertices is allowed to deviate from a regular tetrahedral shape. This structure, symbolized in RCSR as **dia-c3**, has symmetry $I\bar{4}3d$ with nodes in 12a 0, 1/4, 3/8 and links 0, 1/4, 3/8 to 0, 1/4, 1/8. The bond angles are 127° (2×) and 102° (4×). The $I4_1/amd$ net of class I with N = 3 we label **dia-c3***. These two structures are clearly not ambient isotopic as in **dia-c3** each ring is catenated with 14 other rings, but in

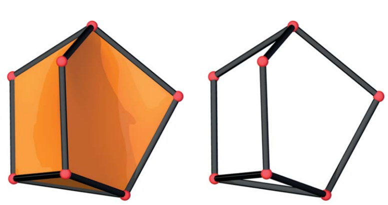

Figure 2
A natural tile of the **lcy** net and its 1-skeleton (right).

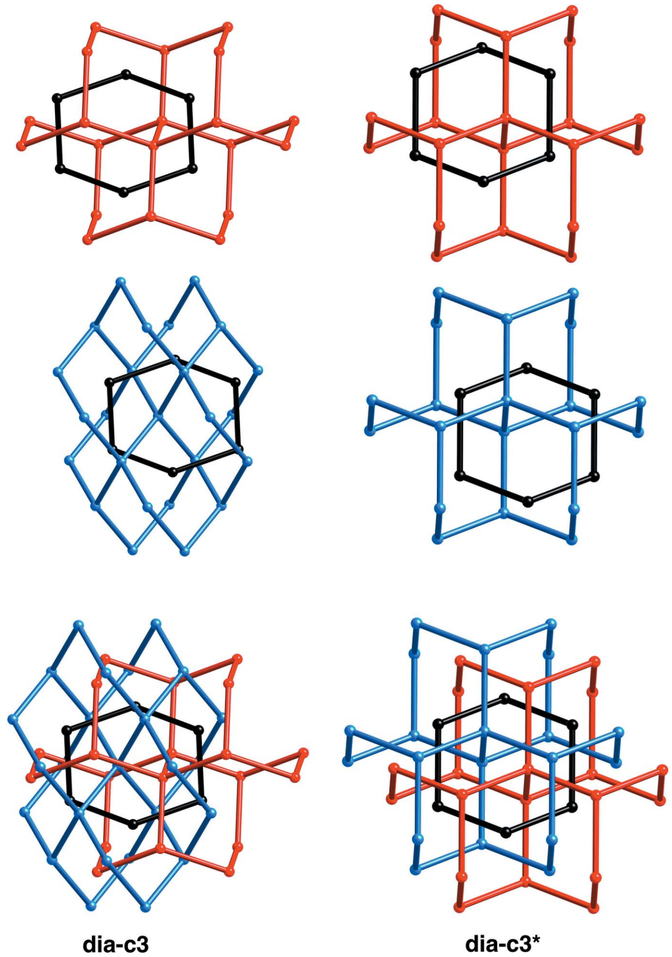

Figure 3
Pattern of catenation of one 6-ring (black) with the rings of other nets (red and blue).

Table 2
Coordinates of nodes and links of interpenetrated **srs** nets with unit link length.

'Number' is the number of rings catenated to a given ring. The nets of **srs-c*** and **srs-c3** do not have full symmetry and have two kinds of node and ring.

N	Class	Space group	*a*, *c*	Node	Link	Number
srs-c	II	$Ia\bar{3}d$	$2^{1/2}$	1/8, 1/8, 1/8	to −1/8, 3/8, 1/8	10
srs-c*	I	$P4_222$	2, $2^{1/2}$	1/4, 0, 0	to 3/4, 0, 0	ring 1 10
					to 0, 1/4, 1/2	ring 2 12
srs-c3	II	$I4_132$	$2(2^{1/2})$	1/8, 3/8, 7/8	to 1/8, 5/8, 5/8	ring 1 16
					to 3/8, 3/8, 1/8	ring 2 20
srs-c4	I	$P4_232$	$1/2^{1/2}$	1/4, 1/4, 1/4	to −1/4, 3/4, 1/4	36
srs-c8	I	$I432$	$1/2^{1/2}$	1/4, 1/4, 1/4	to −1/4, 3/4, 1/4	92
srs-c27	I	$I4_132$	$2(2^{1/2})/3$	1/8, 1/8, 1/8	to 7/8, 5/8, 1/8	364
srs-c54	III	$Ia\bar{3}d$	$2(2^{1/2})/3$	1/8, 1/8, 1/8	to 7/8, 5/8, 1/8	634

dia-c3* each ring is catenated with 12 other rings as shown in Fig. 3. It is worth noting that the three identical nets (say *A*, *B* and *C*) in **dia-c3** are related by a threefold rotation axis. One ring of *A* is catenated to six rings of *B* and eight rings of *C*. There are two 6-rings per vertex and an equal number of *A* rings are catenated to eight rings of *B* and six rings of *C*. Note that there is just one kind of ring in the structure, as all rings are related to others by symmetry operations. A nice example of a crystal structure based on full-symmetry **dia-c3** was reported by Blake *et al.* (1997).

The **ths** net is derived from **dia** by splitting 4-c (4-coordinated) vertices into two 3-c (3-coordinated) ones in a tetragonal fashion and **ths** nets are also commonly found intergrown (Blatov *et al.*, 2004). The symmetry is now $I4_1/amd$. Nodes are in 8*e* 0, 3/4, *z*. There are two kinds of links and three degrees of freedom, so, as commonly done in RCSR, an embedding is found by minimizing the density subject to the constraint of link lengths equal to 1.0. One finds then that $a = 2(2^{1/2})/3$, $c = 8/3$ and $z = 1/32$. Intergrowths of multiple copies (*N*) of this embedding are now to be found as for **dia**. The symmetry for *N* odd is $I4_1/amd$, for *N* twice an odd number, it is $P4_2/nnm$, and for *N* twice an even number, it is $P4/nbm$. *Systre* files for up to $N = 4$ are included in the supporting information. Actually one cannot proceed further with the series without overlap of links along **c**. Overlapping and multiply intergrown **ths** nets observed in practice have less symmetric structures.

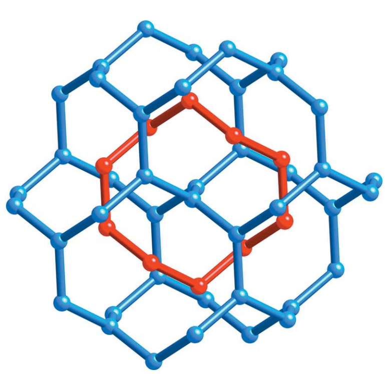

Figure 4
Ten rings catenating one 10-ring (red) in **srs-c**.

3.2. The srs net

The chiral **srs** net is of prime importance in inorganic and materials chemistry (Hyde *et al.*, 2008). It has a self-dual natural tiling and the net of the dual is of opposite hand. The periodic surface separating the two is the gyroid, or *G*, surface, also of prime importance in the structure of materials. As the faces of the tiles are decagons, in such a dual pair each ring is catenated with ten rings of the other net (Fig. 4).

N interpenetrating nets of full symmetry and one hand are possible for *N* = 4, 8 and 27. Data for these are given in Table 2. Nice full-symmetry examples of crystals based on *N* = 4 are described by Kepert *et al.* (2000). For equal numbers of nets with both hands and full symmetry the possibilities appear to be only *N* = 2 or 54. *N* = 2 cases are ubiquitous (Hyde *et al.*, 2008). A spectacular example with *N* = 54 (this is the current record for the number of interpenetrating nets) was reported by Wu *et al.* (2011). In this structure each ring is catenated with 634 others – a fact that should give molecular chemists pause! A fragment of the structure is shown in Fig. 5. The number of catenating rings was determined using *TOPOS* (Blatov *et al.*, 2014).

The patterns of interpenetration are generally quite complicated. In **srs-c4** each ring is catenated with ten rings of two other nets and 16 of the third. In **srs-c8** the pattern is more complicated: each ring is catenated with 92 others – 18 from two nets, 16 from a third and ten from four others – all Hopf links (see also supporting information).

As already noted by Wells (1977), in **srs-c4**, the positions of the nodes are those of a face-centered cubic lattice.

3.3. The qtz and bto nets

The **qtz** net, symmetry $P6_222$, does not have a self-dual tiling, but nevertheless readily intergrows with full symmetry. Copies of the net can be related by translations along the

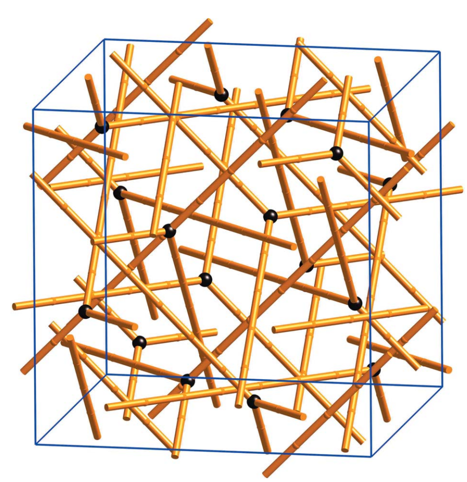

Figure 5
One unit cell of the **srs-c54** structure. Fragments of links are joined to nodes in other unit cells.

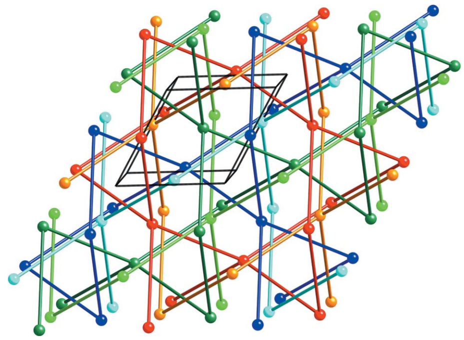

Figure 6
qtz-c6. Each net of the pairs of nets (dark and light blue, dark and light green and red and yellow) are related by translations along the hexagonal **c** direction. Pairs are related by translations along **a**.

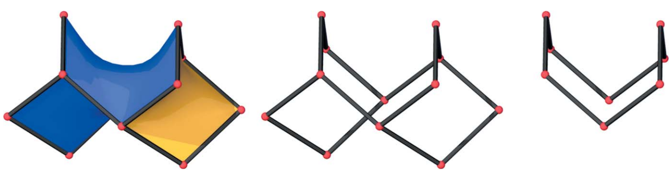

Figure 7
Left a tile of the **qtz** net, center its 1-skeleton, right one 8-ring.

hexagonal **a** or **c** axis or both. To avoid edge intersections, the number of copies related by translations along **c** must not be a multiple of 3. To avoid similar intersections the number related by translations along **a** is limited to 3. Thus with a combination of translations one can have any number of intergrown, non-intersecting **qtz** nets except a multiple of 9. For a given hand of the single **qtz**, say that with symmetry $P6_222$, to preserve the hand with an even number of separate nets, one must use the space group of opposite hand, *i.e.* $P6_422$.

The full-symmetry net has one link and two degrees of freedom (a and c), so in giving data for embeddings, the minimum-density, subject to the constraint of unit link length, conformation is used. For a single net this is $a_1 = (8/3)^{1/2}$, $c_1 = 3^{1/2}$, nodes at 1/2, 0, 0 *etc.* (see Table 3).

A very nice example of a crystal structure with both modes of interpenetration (six nets) was found in $CoAu_2(CN)_4$, in which tetrahedrally coordinated Co atoms are linked by –N–C–Au–C–N– links (Abrahams *et al.*, 1982).[6] Fig. 6 illustrates **qtz-c6**.

The pattern of linking is of some interest. First we note that the **qtz** net has strong 6-rings and three topologically different kinds of strong 8-rings – call the latter 8_a, 8_b and 8_c. Examining the unique proper tiling for **qtz** one finds that only the 8_a rings are used (Fig. 7), so only the 6- and 8_a-rings (one of each per node) are essential. The other 8-rings (two each per vertex) can be expressed as a sum of those essential rings as shown in Figs. 8 and 9. An interesting feature is that the 8-rings are doubly linked (linking number = 2) as shown in Fig. 10 (Delgado-Friedrichs, O'Keeffe & Yaghi, 2005). Single links

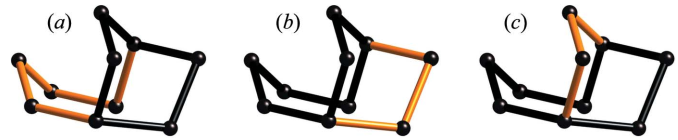

Figure 8
Rings of the **qtz** net. The 8-ring in (*c*) is the sum of a 6-ring (*a*) and a tile 8-ring (*b*). Links that are black in (*c*) are black once in (*a*) and (*b*). Edges that are yellow in (*c*) are black twice in (*a*) and (*b*).

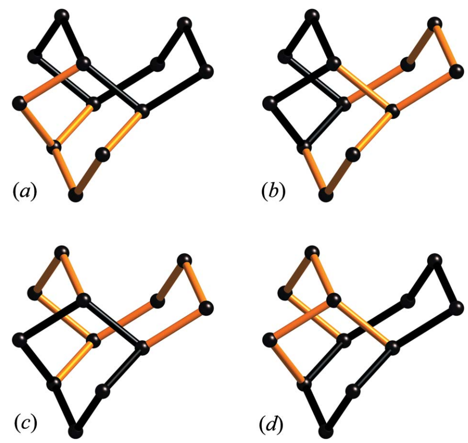

Figure 9
Rings of the **qtz** net. The 8-ring in (*d*) is the sum of a tile 8-ring (*a*) and two 6-rings (*b*) and (*c*). Links that are black in (*d*) are black once in (*a*), (*b*) and (*c*). Links that are yellow in (*d*) are black twice in (*a*), (*b*) and (*c*).

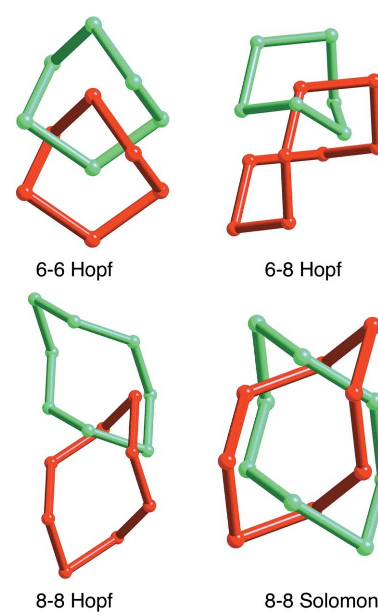

Figure 10
Patterns of catenation in **qtz-c**.

between rings are referred to as Hopf links and double links are referred to as Solomon links (Forgan *et al.*, 2011). In knot theory, knots are classified by the *crossing number*; for the Hopf link this is 2, and for the Solomon link it is 4 (Fig. 9). In all, there are four kinds of catenation:

6-ring with 6-ring 6 Hopf links
6-ring with 8-ring 6 Hopf links

[6] It is interesting to note that the lengthy report of this structure, made 30 years ago by very distinguished crystallographers, makes no mention of interpenetrating nets, nor even of nets at all. Contrast the later discussion of the same structure by Hoskins *et al.* (1995).

Table 3
Coordinates for interpenetrating **qtz** nets with unit link length.

$a_1 = 2(2^{1/2})/3$ and $c_1 = 3^{1/2}$ are unit-cell edges for **qtz**. n and m are integers and s (= ±1) = $-(-1)^{n \bmod 3}$.

N	Space group	a	c	a/c	Node	Link
$n \neq 3m$	$P6_222$	a_1	c_1/n	$(8/3)^{1/2}n$	1/2, 0, 0	to 1/2, 1/2, $-sn/3$
$n \neq 3m$	$P6_422$	a_1	c_1/n	$(8/3)^{1/2}n$	0, 1/2, 0	to 1/2, 1/2, $-sn/3$
$3n \neq 9m$	$P6_222$	$a_1/3^{1/2}$	$3c_1/n$	$[8^{1/2}/9(3^{1/2})]n$	1/2, 0, 0	to 3/2, 1/2, $-sn/3$
$3n \neq 9m$	$P6_422$	$a_1/3^{1/2}$	$3c_1/n$	$[8^{1/2}/9(3^{1/2})]n$	0, 1/2, 0	to 3/2, 1/2, $-sn/3$

8-ring with 8-ring 4 Hopf links

8-ring with 8-ring 2 Solomon links.

In total, there are 18 links per node compared to 12 per node for a diamond catenated pair.

Just as **ths** is derived from **dia**, **bto** is derived from **qtz** by splitting 4-c vertices into two 3-c vertices. In the minimum-density $P6_222$ structure $a = 3^{1/2}$, $c = 9/2$ and nodes are in 1/2, 0, z with z = 1/9. Now the links are to 1/2, 0, $-z$ and 1/2, 1/2, $1/3 - z$. Coordinates for the multiply interpenetrated case are readily derived from the data for **qtz**. Data for **bto-c** and **bto-c3** are given in the supporting information; note again that beyond four nets related by translations along **c**, links parallel to **c** overlap. But **bto-c6** is still possible without overlapping edges (data also in the supporting information).

3.4. The pcu net

The **pcu** net is familiar as the net of the primitive cubic lattice with shortest distances taken as links. A pair of such nets has maximum symmetry $Im\overline{3}m$ and links 0, 0, 0 to 1, 0, 0. The bicontinuous surface separating the two nets is the P minimal surface. For three interpenetrating nets, the best arrangement we find is, with links of length 1.0:

pcu-c3, symmetry $P\overline{3}1m$, $a = (2/3)^{1/2}$, $c = 1/3^{1/2}$. Link 0, 0, 0 to 1, 0, 1, node symmetry $\overline{3}m$.

Here we consider also one pair of fourfold interpenetrating nets (classes II and I, respectively) to illustrate the use of the HRN of Alexandrov *et al.* (2012).

pcu-c4, symmetry $P4_332$, a = 1. Link 1/8, 1/8, 1/8 to 9/8, 1/8, 1/8, node symmetry 32.

pcu-c4*, symmetry $R\overline{3}m$, $a = 2^{1/2}$, $c = 3^{1/2}/4$. Link 0, 0, 0 to 2/3, 1/3, 1/3, node symmetry $\overline{3}m$.

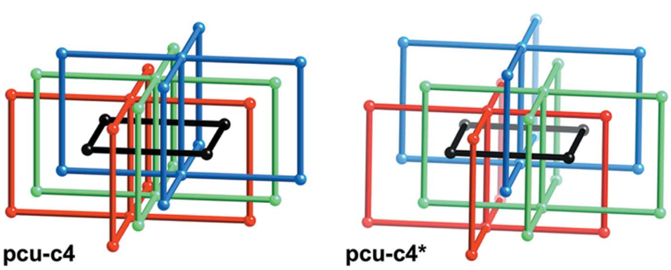

Figure 11
Pattern of catenation of one ring (black) with rings of the other three nets in four interpenetrating **pcu** nets.

As shown in Fig. 11, each ring in each structure is catenated with 12 others, but also it seems clear from the figure that the two nets are not ambient isotopic. In each case the HRN can be obtained by linking the center of the ring to the centers of the catenated rings. When this is done, one finds two distinct 12-c nets, which in fact have the same intrinsic symmetry as the embeddings. *Systre* input files for these two cases are included in the supporting information.

4. Edge-transitive nets with self-dual tilings

Edge-transitive nets are the most important from the point of view of crystal chemistry. We know all the face-transitive (and by duality edge-transitive) proper 3-periodic tilings (Delgado-Friedrichs & O'Keeffe, 2007) and in particular those with self-dual tilings. We list data for the corresponding inter-penetrating nets of a self-dual pair in maximum symmetry in Table 4.

All the tilings in the table, except one, are proper, *i.e.* they have an automorphism group that is the same as that of the nets they carry (Blatov *et al.*, 2007). The exception, which we label **fcu-z**, is a lower-symmetry tiling of **fcu** (the net of the face-centered cubic lattice). The proper tiling of **fcu** consists, of course, of tetrahedra and octahedra. However, if two tetrahedra and an octahedron are glued together, they form a tile with 12 faces of rhombohedral shape. That tile can be used to form a vertex- and edge-transitive, self-dual tiling with symmetry $Pa\overline{3}$ (Dress *et al.*, 1993). So the question arises as to whether two **fcu** nets can interpenetrate (something we believe not to have been observed in practice). The answer is yes, but only without intersecting links if the links are curved (lowering the symmetry from $Fm\overline{3}m$ to $Pa\overline{3}$) as shown in Fig. 12.

A *natural* tiling is a proper tiling with the additional constraint that the tiles are as small as possible, without one

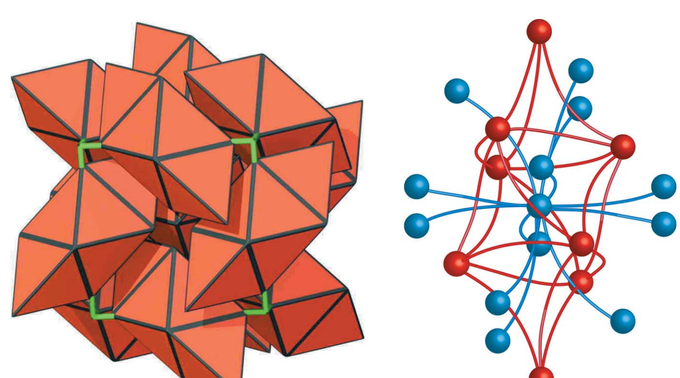

Figure 12
Left: a self-dual tiling by $[3^{12}]$ rhombohedra with $Pa\overline{3}$ symmetry. Right: a fragment of interpenetrating **fcu** nets with curved non-intersecting links. The red links outline one tile with curved edges and a blue node in the center of that tile is linked to its 12 neighbors.

Table 4
Data for self-dual edge-transitive tilings.

CN is coordination number. 'Surface' refers to the symbol of the minimal balance surface symbols taken from Fischer & Koch (1989).

Net	CN	Space group	Link	Tiles	Surface
srs-c	3	$Ia\bar{3}d$	1/8, 1/8, 1/8 – 1/8, 1/8, 1/8	$[10^3]$	*G*
dia-c	4	$Pn\bar{3}m$	1/4, 1/4, 1/4 – 3/4, 3/4, 3/4	$[6^4]$	*D*
pcu-c	6	$Im\bar{3}m$	0, 0, 0 – 1, 0, 0	$[4^6]$	*P*
lcy-c	6	$I4_132$	13/8, 3/8, 3/8 – 1/8, 5/8, 7/8	$[5^6]$	*Y*
fcu-z-c	12	$Ia\bar{3}$	0, 0, 0 – 1/2, 1/2, 0	$[3^{12}]$	
ctn-c	3, 4	$Ia\bar{3}d$	3/8, 0, 1/4 – 0.2083, 0.2083, 0.2083	$4[8^3] + 3[8^4]$	*S*
pyr-c	3, 6	$Ia\bar{3}$	1/2, 1/2, 0 – 0.1667, 0.1667, 0.1667	$2[6^3] + [6^6]$	$C(^{\pm}Y)$
ftw-c	4, 12	$Im\bar{3}m$	0, 0, 0 – 1/1, 1/2, 0	$3[4^4] + [4^{12}]$	$C(P)$
mgc-c	6, 12	$Pn\bar{3}m$	1/2, 1/2, 0 – 3/4, 3/4, 3/4	$2[4^6] + [4^{12}]$	$C(D)$

face being larger than the rest (Blatov *et al.*, 2007). Two further tilings in Table 4 are not natural. In the case of **ctn**, the natural tiling uses two 8-rings (necessarily strong as they are the shortest cycles), say 8_a and 8_b. The natural tiling is $4[8_a^3] + 6[8_a^2.8_b]$. Notice, we use the result below, that 8_b rings are the sum of two 8_a rings, so the 8_a rings form a complete basis set. In the self-dual tiling, pairs of the latter are joined by sharing 8_b faces and now the tiling (self-dual) is $4[8_a^3] + 3[8_a^4]$.

The second non-natural self-dual tiling in the table is that for **lcy**. Now the 3-ring of Fig. 2 is ignored and the tiles are now hexahedra $[5^6]$ as shown in Fig. 13. **lcy** is chiral and the dual tiling has the same hand as the original. In the corresponding intergrown pair (**lcy-c**) of same-chirality nets, the nodes of one are in the centers of the 3-rings of the other (Fig. 14). In a crystal structure, a more favorable conformation, **lcy-c***, is found with pairs of nets of opposite hand and symmetry $Pa\bar{3}$ (Takashima *et al.*, 2010). Now the node is in the center of the $[3.5^3]$ tile and the 3-rings are uncatenated (Fig. 14). Data for these two modes of interpenetration are in the supporting information.

The pattern of catenation in the other pairs of interpenetrating nets is straightforward – there is just one kind of essential *n*-ring that is joined by Hopf links to *n* others. The surfaces separating the pairs of nets are minimal balance surfaces with identifying symbols taken from Fischer & Koch (1989).

We remark that the five vertex- and edge-transitive tilings listed here (for **srs**, **dia**, **pcu**, **lcy** and **fcu-z**) together with the mutually dual pair **bcu** and **nbo** (Delgado-Friedrichs *et al.*, 2003) are a complete list of vertex-, edge-, face- and tile-transitive tilings (*transitivity* 1111).

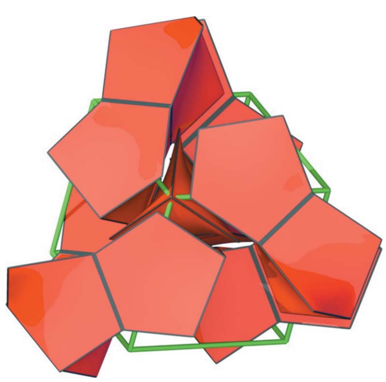

Figure 13
The vertex-, edge-, face- and tile-transitive, self-dual tiling of **lcy**.

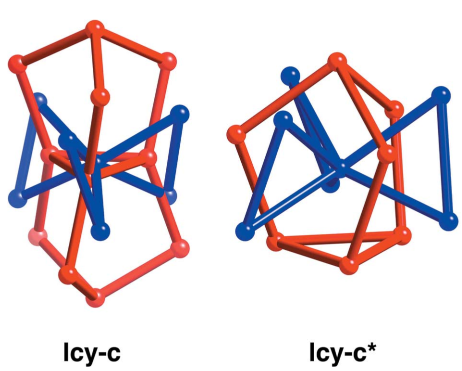

Figure 14
Patterns of interpenetration for **lcy-c** and **lcy-c***.

5. Polycatenated 2-periodic nets

Carlucci *et al.* (2003) prefer the term *polycatenation* to describe *d*-periodic structures derived from linked structures of lower periodicity.[7] Here we briefly describe some uninodal 3-periodic structures formed from 2-periodic nets, specifically the nets of the square lattice, **sql**, and the honeycomb lattice complex, **hcb**. It is an interesting challenge to describe and differentiate the catenations. Carlucci *et al.* (2014) give many examples of occurrences, but not data for maximum-symmetry embeddings; those authors note that 85% of 783 examples of entanglements of 2-periodic structures involved one or the other of these two nets.

Two symmetrical embeddings of **hcb** nets in two (**hcb-c**) and three (**hcb-c3**) orientations (Fig. 15) are for regular hexagons of edge 1:

hcb-c $I4/mcm$, $a = 2/3^{1/2}$, $c = 3^{1/2}$. Node at 1/6, 2/3, 0. Links to −1/6, 1/3, 0 and 1/3, 5/6, 1/2.

hcb-c3 $P6/mcc$, $a = 3$, $c = 3^{1/2}$. Node at 1/2, 2/3, 0. Links to 1/2, 1/3, 0 and 1/2, 5/6, 1/2.

Two symmetrical tetragonal embeddings of **sql** nets with two layers in the repeat unit are (Fig. 16):

sql-c $P4_2/mmc$, $a = 1$, $c = 1$. Node at 0, 1/2, 0. Links to 1, 1/2, 0 and 0, 1/2, 1.

sql-c* $I4/mcm$, $a = 1$, $c = 2^{1/2}$. Node at 0, 1/2, 0. Link to 1/2, 0, 1/2.

Two symmetrical hexagonal embeddings of **sql** nets with three layers in the repeat unit are (Fig. 17):

[7] Multiply linked catenanes are more generally called *polycatenanes* (*e.g.* Niu & Gibson, 2009) but also (and linguistically more correct) *multicatenanes* (*e.g.* Wang *et al.*, 2004). We reluctantly accept the more common *polycatenation*.

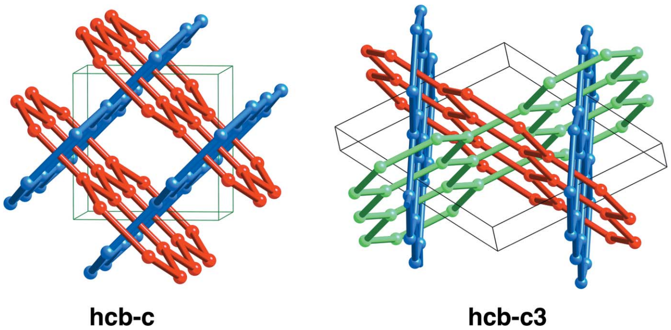

Figure 15
Two symmetrical embeddings of polycatenated **hcb** nets.

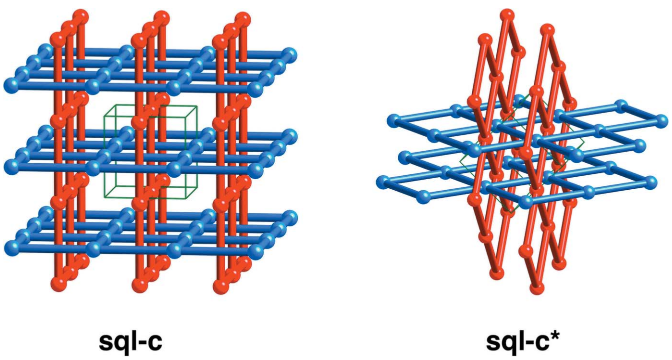

Figure 16
Two tetragonal modes of polycatenation of two sets of **sql** (square lattice nets).

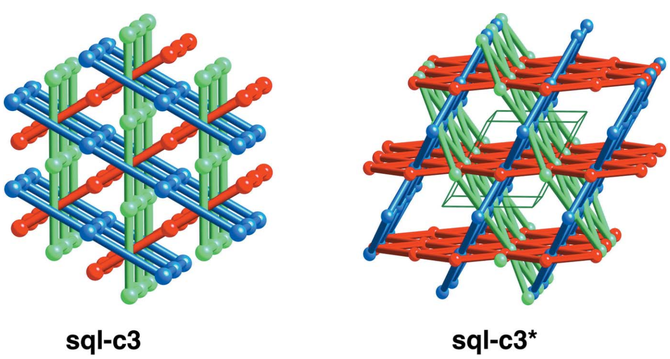

Figure 17
Two hexagonal modes of polycatenation of three sets of **sql** (square lattice nets).

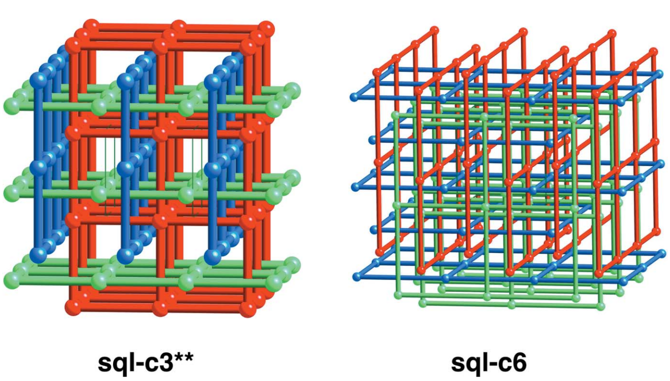

Figure 18
Two rhombohedral patterns of polycatenated **sql** nets.

sql-c3 $P6_222 = 1$, $c = 1$. Node at 1/2, 0, 0. Links to 3/2, 0, 0 and 1/2, 0, 1.

sql-3c* $P6/mcc$, $a = 2^{1/2}$, $c = 2^{1/2}$. Node at 1/2, 0, 0. Link to 1/2, 1/2, 1/2.

Two rhombohedral patterns with three families of **sql** nets mutually perpendicular to each other (Fig. 18):

sql-c3**, $R3$, $a = 1$, $\alpha = 90°$. Node at 0, 1/3, 2/3. Links to 1, 1/3, 2/3 and 0, 4/3, 2/3.

sql-c6, $R3c$, $a = 1$, $\alpha = 90°$. Node at 0, 1/3, 2/3. Links to 1, 1/3, 2/3 and 0, 4/3, 2/3.

6. A note on self-entanglement

In a 3-periodic net, there are an infinite number of cycles and one can always find a pair of cycles that forms a link or knot or some other kind of entanglement. In that not very useful sense, all nets are self-entangled. At the other extreme, if one considers just the essential rings of the structure, nets such as **coe** (the net of the coesite form of silica) commonly described as self-catenated (*e.g.* O'Keeffe, 1991) are not self-entangled as the catenated rings are not essential (**coe** admits a natural tiling).

Another example cited by Delgado-Friedrichs, Foster *et al.* (2005) is the net **fnu**. This 5-c net can be derived by linking a pair of diamond nets (**dia-c**) by an extra edge. The resulting structure has only 6-rings, but, as shown by Blatov *et al.* (2007), 6-rings that are not part of the original set of catenated 6-rings of **dia-c** can be used to construct a tiling, and the *essential* rings are not catenated.

Yet another example of a net constructed from **dia-c** is **ddi**. This 8-c net has the catenated 6-rings of **dia-c** and indeed was called a 'self-penetrated' and a 'polyrotaxane' (Yang *et al.*, 2009). However, the vertices are linked by four more edges

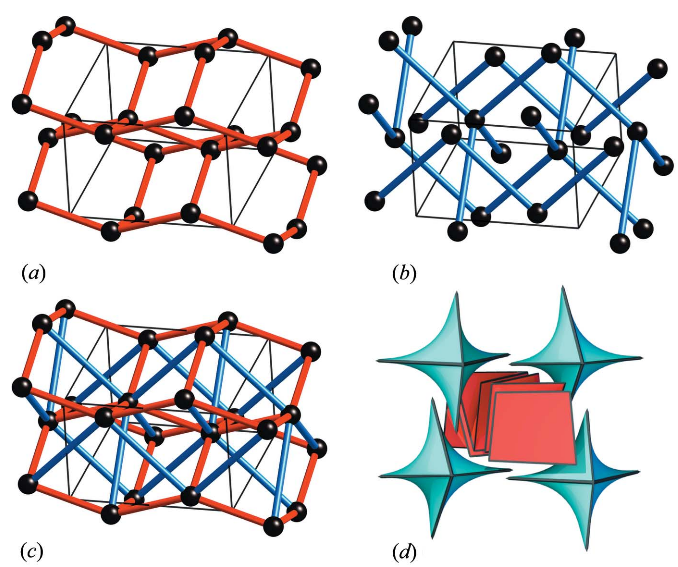

Figure 19
Aspects of the net **ddi**. (*a*) A **dia net**. (*b*) Two interpenetrating **dia** nets linking the same vertices as in (*a*). (*c*) The nets in (*a*) and (*b*) combined. (*d*) Part of a natural tiling of **ddi**. All tile faces are 4-rings. Red tiles are $[4^3]$.

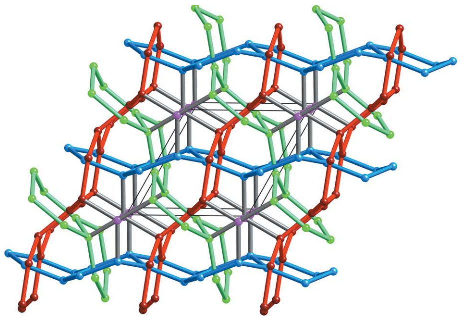

Figure 20
The **jcy** net. Blue, green and red parts are **hcb-c3** (*cf.* Fig. 15). Magenta nodes and gray links join the **hcb** nets into one connected net.

that form another **dia** net as shown in Fig. 19. The result is that now all the strong rings are 4-rings and two of them serve as faces of the natural tiling. It can readily be verified that the two 4-rings form a complete basis, so again the essential rings are not catenated. From the tiling in the figure, it may be seen that the $[4^4]$ tiles include non-essential 4-rings that are the sum of two edge-sharing faces. The 6-rings are the sum of at least three 4-rings, so they are weak rings.

It does seem paradoxical in these last two examples that adding more links to a catenated structure (**dia-c**) results in a structure we no longer consider self-catenated. At the same time, considering only the essential rings does also seem the most logical criterion for self-entanglement.

If the layers of **hcb-c3** are linked to additional nodes, each linked to three **hcb** nets, a net (**jcy**) is obtained in which *all* the strong rings (one each of 6-ring and 8-ring) in the structure are catenated with other rings (Fig. 20). This serves as the underlying net of the metal–organic framework ZJU-28 (Yu *et al.*, 2012). Now there are no uncatenated rings in the structure, which is a single net (connected), so surely this one can be considered self-catenated. Perhaps we should call such structures *essentially* self-catenated.

The levels of self-catenation may be summarized as follows:

Cycles, not rings, catenated – trivial.

Weak rings catenated – *e.g.* **ddi**.

Strong, non-essential, rings catenated – *e.g.* **fnu**.

Essential rings catenated – essentially self-catenated, *e.g.* **jcy**.

This work is supported by the US National Science Foundation, grant DMR 1104798. We acknowledge helpful correspondence and advice on *TOPOS* from Professors V. A. Blatov and D. M. Proserpio. We are grateful to a referee for an unusually thorough and helpful reading.

References

Abrahams, S. C., Zyontz, L. E. & Bernstein, J. L. (1982). *J. Chem. Phys.* **76**, 5458–5462.
Alexandrov, E. V., Blatov, V. A., Kochetkov, A. V. & Proserpio, D. M. (2011). *CrystEngComm*, **13**, 3947–3958.
Alexandrov, E. V., Blatov, V. A. & Proserpio, D. M. (2012). *Acta Cryst.* A**68**, 484–493.
Batten, S. R. & Robson, R. (1998). *Angew. Chem. Int. Ed.* **37**, 1460–1494.
Blake, A. J., Champness, N. R., Khlobystov, Y. N., Lemonovskii, D. A., Li, W.-S. & Schröder, M. S. (1997). *Chem. Commun.* pp. 1339–1340.
Blatov, V. A., Carlucci, L., Ciani, G. & Proserpio, D. M. (2004). *CrystEngComm*, **6**, 377–395.
Blatov, V. A., Delgado-Friedrichs, O., O'Keeffe, M. & Proserpio, D. M. (2007). *Acta Cryst.* A**63**, 418–425.
Blatov, V. A., Shevchenko, A. P. & Proserpio, D. M. (2014). *Crystal Growth Des.* **14**, 3576–3586.
Bragg, W. H. & Bragg, W. L. (1915). *X-rays and Crystal Structure*, p. 155. London: G. Bell and Sons.
Carlucci, L., Ciani, G. & Proserpio, D. M. (2003). *Coord. Chem. Rev.* **246**, 247–289.
Carlucci, L., Ciani, G., Proserpio, D. M., Mitina, T. G. & Blatov, V. A. (2014). *Chem. Rev.* **114**, 7557–7580.
Castle, T., Evans, M. E. & Hyde, S. T. (2011). *Prog. Theor. Phys.* **111**, 235–244.
Delgado-Friedrichs, O. (2005). *Discr. Comput. Geom.* **33**, 67–81.
Delgado-Friedrichs, O., Foster, M. D., O'Keeffe, M., Proserpio, D. M., Treacy, M. M. & Yaghi, O. M. (2005). *J. Solid State Chem.* **178**, 2533–2554.
Delgado-Friedrichs, O., Hyde, S. T., Mun, S.-W., O'Keeffe, M. & Proserpio, D. M. (2013). *Acta Cryst.* A**69**, 535–542.
Delgado-Friedrichs, O. & O'Keeffe, M. (2005). *J. Solid State Chem.* **178**, 2480–2485.
Delgado-Friedrichs, O. & O'Keeffe, M. (2007). *Acta Cryst.* A**63**, 344–347.
Delgado Friedrichs, O., O'Keeffe, M. & Yaghi, O. M. (2003). *Acta Cryst.* A**59**, 22–27.
Delgado-Friedrichs, O., O'Keeffe, M. & Yaghi, O. M. (2005). *Solid State Sci.* **5**, 73–78.
Dress, A. W. M., Huson, D. H. & Molnár, E. (1993). *Acta Cryst.* A**49**, 806–817.
Evans, N. H. & Beer, P. D. (2014). *Chem. Soc. Rev.* **43**, 4658–4683.
Ewald, P. P. & Hermann, C. (1931). *Strukturbericht 1913–1928.* Leipzig: Akademische Verlagsgesellschaft MBH.
Fischer, W. & Koch, E. (1989). *Acta Cryst.* A**45**, 726–732.
Forgan, R. S., Sauvage, J. P. & Stoddart, J. F. (2011). *Chem. Rev.* **111**, 5434–5464.
Goetzke, K. & Klein, H. (1991). *J. Non-Cryst. Solids*, **127**, 215–220.
Hoskins, B. F., Robson, R. & Scarlett, N. V. Y. (1995). *Angew. Chem. Int. Ed. Engl.* **34**, 1203–1204.
Hyde, S. T. & Delgado-Friedrichs, O. (2011). *Solid State Sci.* **13**, 675–683.
Hyde, S. T., O'Keeffe, M. & Proserpio, D. M. (2008). *Angew. Chem. Int. Ed.* **47**, 7996–8000.
Kepert, C. J., Prior, T. J. & Rosseinsky, M. J. (2000). *J. Am. Chem. Soc.* **122**, 5158–5168.
Koch, E., Fischer, W. & Sowa, H. (2006). *Acta Cryst.* A**62**, 152–167.
Lee, C. J., Kang, Y. M., Cho, K. H. & No, K. T. (2009). *Proc. Natl Acad. Sci. USA*, **106**, 17355–17358.
Moreira de Oliveira, M. Jr & Eon, J.-G. (2014). *Acta Cryst.* A**70**, 217–228.
Niu, Z. & Gibson, H. W. (2009). *Chem. Rev.* **109**, 6024–6046.
O'Keeffe, M. (1991). *Z. Kristallogr.* **196**, 21–37.
O'Keeffe, M., Peskov, M. A., Ramsden, S. J. & Yaghi, O. M. (2008). *Acc. Chem. Res.* **41**, 1782–1789.
Reineke, T. M., Eddaoudi, M., Moler, D., O'Keeffe, M. & Yaghi, O. M. (2000). *J. Am. Chem. Soc.* **122**, 4843–4844.
Schröder-Turk, G. E., de Campo, L., Evans, M. E., Saba, M., Kapfer, S. C., Varslot, T., Grosse-Brauckmann, K., Ramsden, S. & Hyde, S. T. (2013). *Faraday Discuss.* **161**, 215–247.
Takashima, Y., Bonneau, C., Furukawa, S., Kondo, M., Matsuda, R. & Kitagawa, S. (2010). *Chem. Commun.* **46**, 4142–4144.

Uribe-Romo, F. J., Hunt, J. R., Furukawa, H., Klöck, C., O'Keeffe, M. & Yaghi, O. M. (2009). *J. Am. Chem. Soc.* **31**, 1570–1571.
Wang, L., Vysotsky, M. O., Bogdan, A., Bolte, M. & Böhmer, V. (2004). *Science*, **304**, 1312–1314.
Wasserman, E. (1960). *J. Am. Chem. Soc.* **82**, 4433–4434.
Wells, A. F. (1977). *Three-Dimensional Nets and Polyhedra.* New York: Wiley.
Wu, H., Yang, J., Su, Z. M., Batten, S. R. & Ma, J. F. (2011). *J. Am. Chem. Soc.* **133**, 11406–11409.
Yang, G., Lan, Y., Zang, H., Shao, K., Wang, X., Su, Z. & Jiang, C. (2009). *CrystEngComm*, **11**, 274–277.
Yu, J., Cui, Y., Wu, C., Yang, Y., Wang, Z., O'Keeffe, M., Chen, B. & Qian, G. (2012). *Angew. Chem. Int. Ed.* **51**, 10542–10545.